VII. GEOPHYSICAL RESEARCH

A. High Magnetic Fields*

Academic and Research Staff

Prof. F. Bitter
Prof. G. Fiocco

Graduate Students

S. J. Bless

1. PRELIMINARY EXPERIMENTS WITH A FAST Z-PINCH CAPACITOR DISCHARGE: THE GENERATION OF HIGH PRESSURES IN SOLIDS

Preliminary experiments are being carried out to study the application of a fast capacitor Z-pinch discharge to the generation of high magnetic fields, dense vaporized metal plasmas, and high pressures. These experiments bear on aspects of the relatively well-known exploding wire technology, although most previous efforts in that field appear to us not to have been primarily directed toward the areas of interest mentioned here.

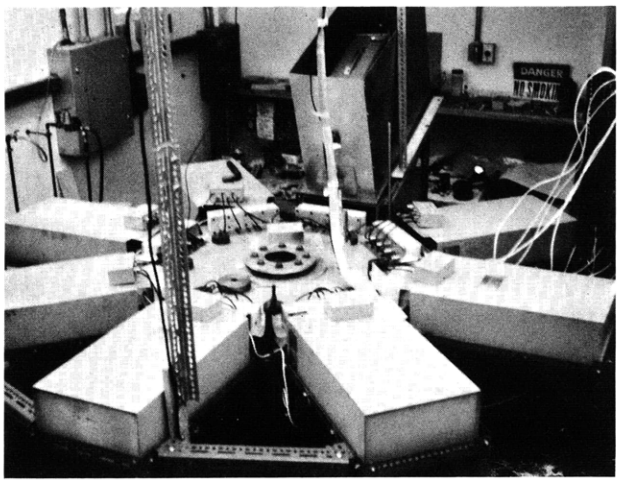

Fig. VII-1.
Photograph of the apparatus.

The apparatus (Fig. VII-1) consists of 8 capacitor and spark-gap assemblies radially connected to an octagonal isolated set of plates. The plates are low-inductance transmission lines feeding a centrally located connecting rod, 1 inch long. During the

*This work is supported in part by the Joint Services Electronics Programs (U.S. Army, U.S. Navy, and U.S. Air Force) under Contract DA 28-043-AMC-02536(E).

discharge, current up to several million amperes passes through the rod, thereby generating in its immediate vicinity a megagauss toroidal magnetic field. The passage of the current subjects the rod to a pressure that may amount to hundreds of kilobars. Also, the material of the rod may sublime, thereby becoming a dense metallic plasma.

In particular, the capacitor bank has the following characteristics: 8 Tobe-Deutschmann 15-μf, 3000-joule, 20-kV low-inductance capacitors Model ESC 248F, triggered by 8 spark-gap pulsers Tobe Deutschmann Model TG1, and a 100-kV, 30-ma high-voltage power supply, DEL Electronics Corporation Model PS100-30-3.

The octagonal feeding plates are 15 inches on a side, 3/8 inch thick, and are separated by mylar sheets of 0.060-inch thickness. The central portion of the plates can be disassembled to allow easy substitution of the center rod and replacement of the central insulation when necessary. The rod is enclosed in a chamber, 7.15 mm in diameter. The ringing period of the system, short-circuited by the rod, is approximately 4 μsec.

A modest amount of instrumentation complements the bank. There is a Science Accessories Corporation voltage divider Model 003, for voltage waveform measurements, loops for current measurements, and other instrumentation to monitor the charge on the capacitors and the light output of the explosion. The various pickups are brought through coaxial cables to a screened cage for oscilloscopic display.

At this time, we are reporting some initial tests designed primarily to demonstrate the production of high pressures.

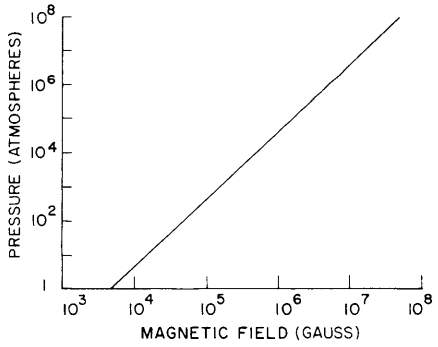

Fig. VII-2. Relationship between magnetic flux and pressure.

By equating $p = \frac{B^2}{2\mu_o}$ we expect that relatively high pressures would be generated at the interface between the magnetic field and the conducting material. A graph displaying this well-known relation is shown in Fig. VII-2. The range of operation of our device is of the order of 1 mG for the magnetic field intensity, and of the order of 10^5 atm for the resultant pressure. Precise figures depend essentially on the dimensions of the current-carrying rod and the modality of the discharge; in particular, on the fraction of current

which may not be confined to the rod, because of a surrounding plasma. The maximum magnetic field that would be expected in the event that all the current are carried by the rod of diameter d is

$$B = \frac{4 \times 10^{-4} I}{d} \quad \text{(MKS units)}.$$

Most of our experiments have been with 4-mm diameter iron rods, but we have also used a few stainless-steel and molybdenum rods of various sizes.

From a knowledge of the charge stored and the discharge time, we believe that the maximum current carried, at least partially, by a 4-mm diameter rod was 2.7×10^6 amps; however, the rod was entirely vaporized. The maximum current that a 4-mm diameter rod would carry without apparent damage was 1.9×10^6 amps, which would correspond to a magnetic field at the periphery of the rod of 1.9×10^6 Gauss.

In some cases, rods have been confined in boron nitride cylinders: the highest current we have passed through a confined rod is 1.6×10^6 amps through a 2.1-mm stainless-steel rod, which would correspond to a magnetic field of $\sim 3 \times 10^6$ Gauss. As a result, the rod was vaporized and the boron nitride was shattered.

In order to establish the achievement of high pressures in the samples, we have

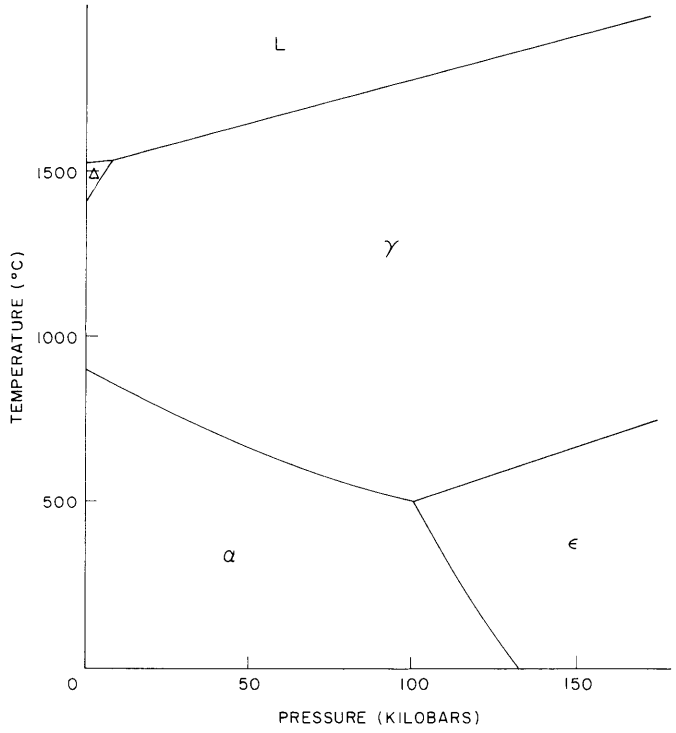

Fig. VII-3. Phase diagram of iron.

carried out experiments with 4-mm diameter Armco iron rods. The object of the experiments was to demonstrate the formation of the high-pressure phase of iron, which occurs in shock experiments at 130 kilobars (see Fig. VII-3).

In our experiments we are limited to the study of samples that can be recovered. The response of the rods to various capacitances and voltages is shown in Fig. VII-4. The

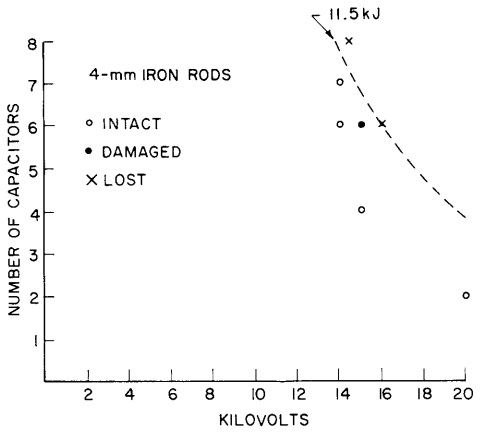

Fig. VII-4. Response of 4-mm iron rods.

maximum pressure expected without damage to the rod is ~160 kilobars achieved with 7 capacitors at approximately 14 kV.

The microhardness of the recovered rods was measured, and a typical profile is shown in Fig. VII-5. In general, the hardness across the rods was often low in the

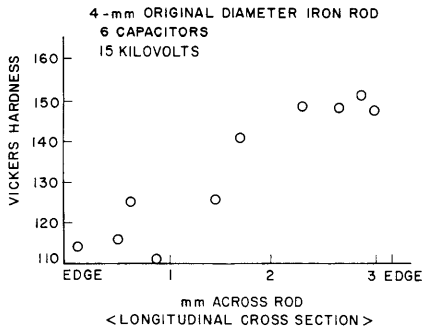

Fig. VII-5. A typical hardness profile.

center, and was usually very lopsided with a great deal of scatter in the measurements.

The original stock, however, was also somewhat softer in the center. A stock rod had a Vickers hardness of 155 + 12 near the edge, and 148 ± 9 near the center. (The ± quantity is the standard deviation.) All of the fired samples had hardness less than this. Some were even below 140, so there is no doubt that the effect of the discharge was to make the rods less hard.

The irregular grain boundaries and internal grain structure produced by the discharge strongly suggest that a phase change took place. Figures VII-6 and VII-7 are 'before' and 'after' metallographs that illustrate these effects.

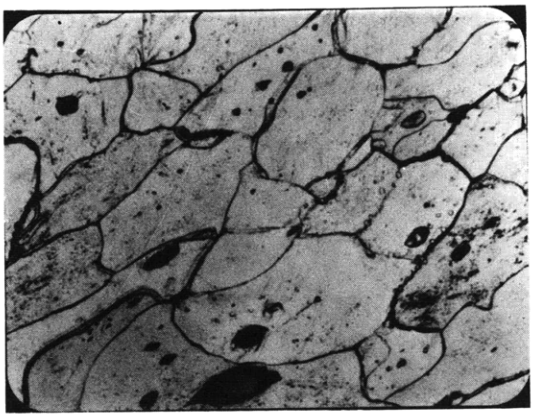

Fig. VII-6. Stock Armco iron rod, 200X.

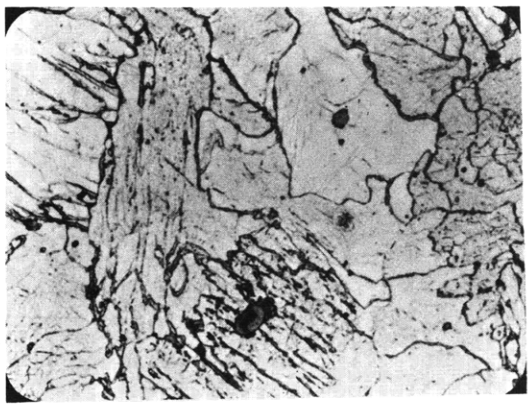

Fig. VII-7. Iron rod after discharge of 6 capacitors at 15 kV (cross section normal to current flow), 200X.

Such structures also resemble those obtained by quenching iron from the high-temperature γ phase. It seems unlikely that sufficient heat to induce the γ-phase transition could have flowed into the rod, since the rod is only in contact with the hot conducting region for a few tens of microseconds (exhaust ports allowed the vapor to dissipate). Also, the mechanism for quenching is open to question; thus, it is possible that a change to the ϵ phase took place. The experiments are now being continued. We are planning shots with annealed iron, which has a more regular grain structure, and with materials of geophysical interest, starting with quartz.

F. Bitter, S. J. Bless, G. Fiocco

VII. GEOPHYSICAL RESEARCH

B. Upper Atmospheric Physics*

Academic and Research Staff

Prof. G. Fiocco
Dr. G. W. Grams

Graduate Students

J. B. DeWolf
D. F. Kitrosser
H. C. Koons

1. OPTICAL RADAR OBSERVATIONS OF MESOSPHERIC AEROSOLS IN NORWAY DURING THE SUMMER 1966

In the summer of 1966, an optical radar was operated in the vicinity of Oslo, Norway, to obtain measurements of the aerosol content of the mesosphere at times when noctilucent clouds might be present. This work was a continuation of similar experiments conducted in Alaska and Sweden in the summer of 1964.

The observations have provided a measurement of the backscattering cross section of noctilucent clouds, and seem to confirm our earlier results, thereby indicating that the altitude region 60-70 km contains an appreciable amount of particulate material during noctilucent cloud (NLC) displays.

Description of the Experiments

In the summer of 1964, optical radar experiments were performed in Alaska and Sweden for the purpose of observing the mesospheric aerosol content during noctilucent cloud displays.[1]

These preliminary experiments allowed us to measure an average scattering cross section of stratifications at altitudes near 70 km. The NLC activity during the summer of 1964 was moderate, however, and we were not able to operate the optical radar during conditions when NLC displays were visible overhead. The presence of a layer at 70 km, well below the height commonly found for NLC's was taken as an indication that measurable processes involving a wide range of mesospheric heights might be involved.

In order to acquire further observational evidence, a new series of experiments was carried out at Kjeller (60.0°N, 11.0°E) near Oslo during the summer of 1966. Thanks to the hospitality of the Norwegian Defence Research Establishment, it was possible to

*This work was supported principally by the National Aeronautics and Space Administration (Grants NGR-22-009-131 and NGR-22-009-114, and Contract NAS 12-436).

operate the device at a location very near 60° of latitude, and yet have the advantages of the proximity to an equipped laboratory.

Latitude 60° is recognized to offer the highest probability of visually detecting the clouds and is probably also the best location for optical radar observations with apparatus at the present level of development. While a more southerly location would increase the length of the interval of darkness for observations, it might reduce the probability of having clouds overhead.

The apparatus, installed in a trailer, was basically the same as the optical radar unit used in Sweden in the summer of 1964, although a few improvements were incorporated to improve the reliability and performance of the system. For instance, a temperature-controlled refrigerator was used to maintain the laser unit and the narrow-band interference filters at constant temperature, with a closed-loop circulation of distilled water. A polarizing filter was included in the receiver to minimize the twilight sky background. The filter was adjusted to accept only the linearly polarized radiation emitted by the laser. Since the observations were carried out at the zenith, the laser and telescope were fixed to a mount that could be rotated around the vertical axis to reduce the polarized sky background to a minimum.

Other improvements in the laser itself provided approximately 2-joule pulses of less than 100-nsec duration at a maximum p.r.f. of 0.5 sec^{-1}. To record the data, the apparatus utilized a 556-BH1 automatic radarscope camera, modified for use on a Tektronix 555 dual-beam oscilloscope. Two traces, displaying the amplified photomultiplier current, were recorded simultaneously with different sweep rates: one trace recorded the echoes from 0-200 km altitude for the noctilucent cloud data, the other displayed either the echoes from 0-40 km, to obtain profiles of the stratospheric aerosol layer, or expanded records of the 60-90 km height region.

A discussion of the 0-40 km data, which we hope will supplement previous work,[2,3] will not be presented at this time.

In addition to the optical radar instrumentation, a developmental airglow photometer, which was described in Quarterly Progress Report No. 85 (page 49), was also mounted in the trailer to measure the intensity and the rotational temperature of the OH emission from the mesosphere.

Summary of Observations

The nights during which observations were made and for which data have been reduced are given in Table VII-1. The table also indicates whether or not NLC's were visually observed during the night; in particular, "overhead" refers to an NLC display that for some portion of the night, always rather brief, could be seen overhead. "Strong" indicates a night when clouds were visible at elevation angles exceeding 20°: in these situations the clouds usually covered a large portion of the sky but did not extend

overhead. "Weak" is used to designate those nights when clouds could be seen low on the horizon. It is possible that, on some of these dates, clouds might have been present but were not observed visually because of local visibility conditions.

Table VII-1. Nights when reliable observations were made and reduced.

JUNE 1966		JULY 1966	
11-12	No NLC	18-19	Strong
16-17	No NLC	19-20	Overhead
30-1 July	Overhead	20-21	No NLC
		21-22	No NLC
JULY 1966		22-23	No NLC
2-3	Weak	26-27	Weak
6-7	Overhead		
7-8	No NLC		
13-14	Strong	AUGUST 1966	
17-18	No NLC	15-16	Strong

The greater part of the data were recorded on 0-200 km traces. Although the apparatus is, in principle, capable of very high range resolution (a few tens of meters), the storage and further reduction of the data largely limits the high instrumental resolving power. We also note that an uncertainty in the range determination may result from any inaccuracy with which, during the data reduction, the time of pulse transmission is located: the range determinations are considered to be accurate to the nearest kilometer. When the 200-km records are reduced, the measured range for each observed photoelectron is considered to be correct to the nearest kilometer. Most of these digitized records were analyzed by counting the total number of photoelectrons received from 2-km range intervals during the period of observation.

Figure VII-8 summarizes observations carried out on nights when NLC's were present (nights designated "strong" or "overhead" in Table VII-1). The figure indicates the total number of photoelectrons obtained in successive 2-km intervals between 40 and 100 km. The noise level (dark-current and sky background) was established by averaging the returns between 80 and 100 km; the estimated best fit for a molecular atmosphere, with noise taken into account, is shown by the dashed curve. Error flags have a total extent equal to $2\sqrt{n}$, where n is the number of counts at each altitude, and give an indication of the statistical relevance of the count. A small increase in cross sections is evident for the records when noctilucent clouds were overhead, and it is taken to be their echo. Also shown is an enhancement in the

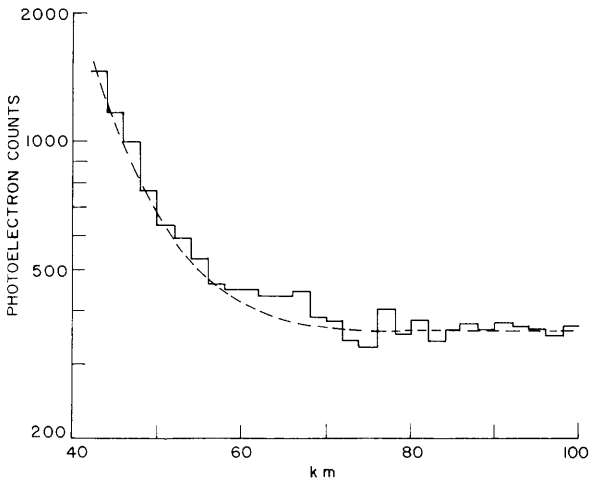

Fig. VII-8. Sum of observations obtained during noctilucent cloud displays.

returns from 60 to 70 km. This excess signal is presumably due to the presence of a considerable amount of particulate material, since at those heights no condensation of water vapor is possible.[4,5]

Figure VII-9 shows a similar summation for all days when no NLC's were present. Many of these dates were early in June, and are affected by larger amounts of noise, as evidenced by the shape of the curve. A possible increase in signal between 50 and 60 km is discernable, although not as evident as in Fig. VII-8; there is no visible increase in the 60-70 km region.

To give some evidence to the daily variation of the scattering cross section, we have grouped each night's data into 10-km intervals. A reference noise level has then been

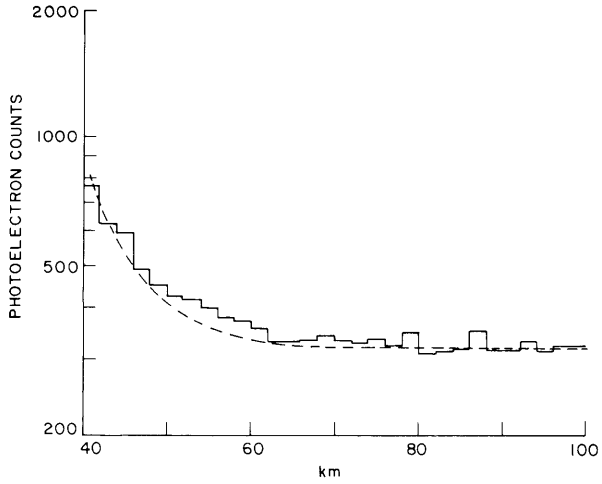

Fig. VII-9. Sum of observations obtained when noctilucent clouds were not visible.

computed by taking the average output between 90 and 140 km, and has been subtracted from the returns at lower heights. The remainder, for each 10-km interval, has then been compared with the returns that would be expected from a molecular atmosphere. If we call Σ the observed radar cross section per unit volume of the atmosphere and Σ_M the cross section expected from a clear molecular atmosphere, then the quantity $(\Sigma/\Sigma_M)-1$ represents the excess scattering attributable to aerosols. Unfortunately, our measurements do not yield an absolute value for the cross section at each altitude, because of the difficulty in determining a constant in the radar equation that relates the number of photoelectrons received from a scattering layer to its radar cross section. We evaluate this radar constant, however, by assuming that there is some altitude interval for which backscattering by aerosols can be neglected, and the cross section for that region is then taken to be equal to the molecular cross section ($\Sigma/\Sigma_M = 1$). With the lack of better information, we have chosen the 40-50 km altitude interval as the

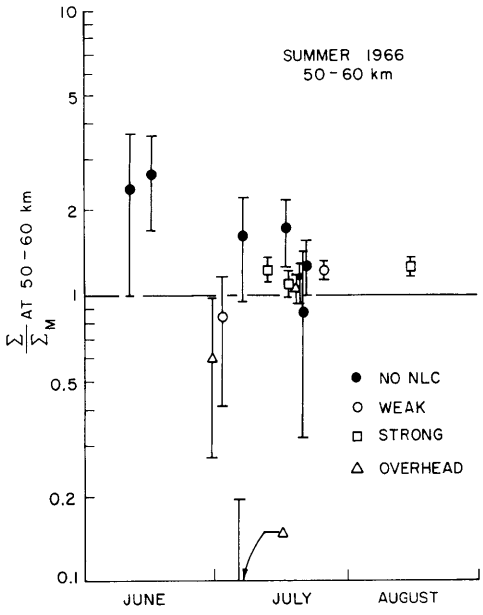

Fig. VII-10. Daily variations of the average scattering ratio for the 50-60 km region.

calibration region. All scattering ratios have therefore been normalized to this altitude interval: Higher altitudes exhibit considerably more fluctuation than this region, while lower altitudes have a high density of photoelectron pulses on each record so that it becomes possible for a nonlinearity in the counting technique to be introduced by the chance that two or more pulses may occur so close together that they might not be recognized as more than one photoelectron on the record.

Under the assumption, therefore, that the returns from the 40-50 km region have a negligible component from aerosols, we have computed scattering ratios

for various altitude regions for days when reliable observations have been made and have been analyzed. Figure VII-10 illustrates the daily variation of the scattering ratio in the 50-60 km region. Figure VII-11 shows the ratios for 60-70 km region. These graphs

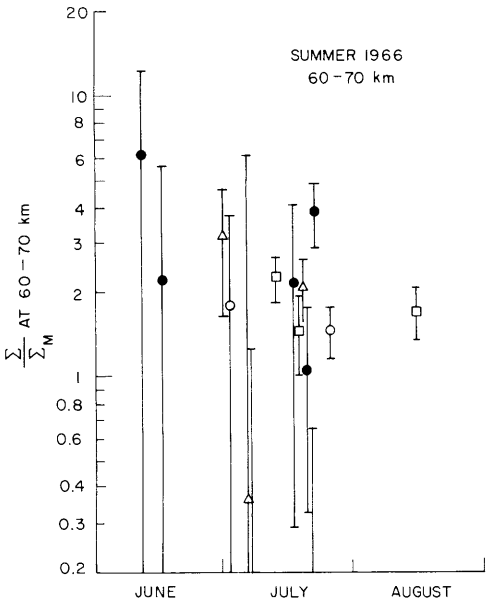

Fig. VII-11. Daily variations of the average scattering ratio for the 60-70 km region.

indicate the same general trend displayed in Figs. VII-8 and VII-9. Increased dust amounts are evident in the 50-60 km region when NLC's were not observed visually, and in the higher region, 60-70 km, when strong NLC displays were observed.

Since it is difficult to resolve two closely spaced pulses on the 0-200 km traces when the range differential is less than 1 km, it is possible that some pulses might be missed when digitizing the records, especially for the case of strong echoes from geometrically thin layers. For this reason, expanded traces were sometimes recorded for detailed studies of thin scattering layers. These records enable us to study the returns from ~0-90 km altitude with a range resolution of ~100 meters.

On 6-7 July, 60-90 km records were obtained during a strong noctilucent cloud display. Visual observations indicated that the cloud was approaching from a northerly direction and appeared to be directly overhead just before dawn. Figure VII-12 gives the results on the analysis of these high-resolution data. Curve a shows all of the photoelectron counts in 1-km intervals during the period immediately before the arrival of the cloud, and curve b shows all subsequent counts for each range interval. A strong scattering layer at 74 km was associated with the noctilucent cloud; the optical thickness of this layer was calculated to be 10^{-4} during the time that the noctilucent cloud was overhead.

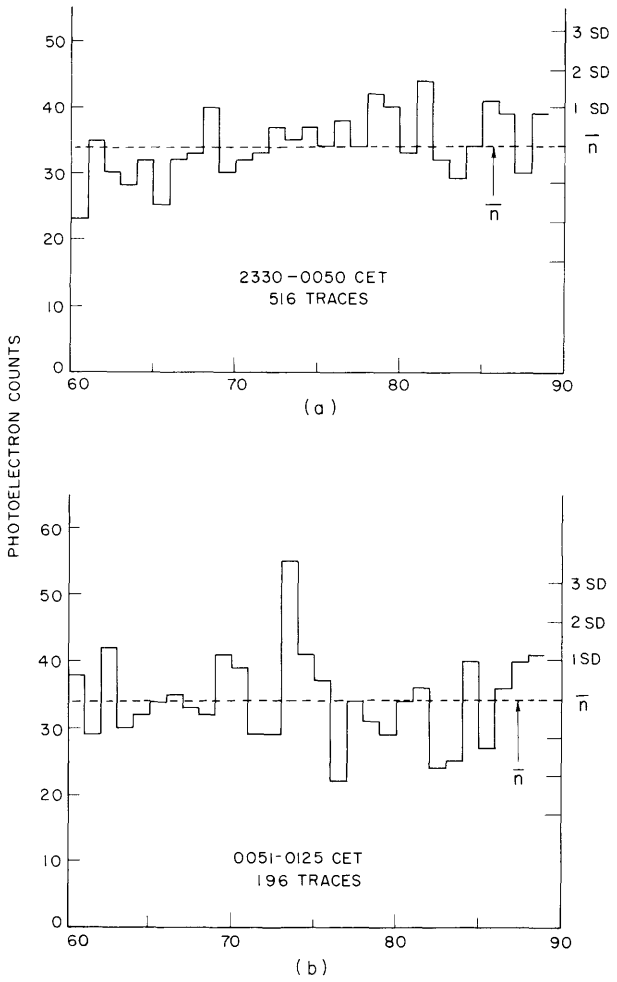

Fig. VII-12. Detailed 60-90 km observations summed over 1 km altitude intervals for 6-7 July. Curve a: sum of observations before the arrival of the noctilucent cloud. Curve b: sum of observations after the cloud appeared to be overhead.

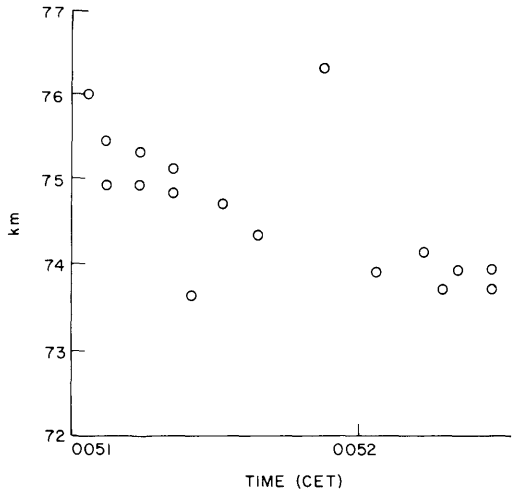

Fig. VII-13.

Detailed study of the height variation of the overhead cloud observed on 6-7 July 1966. Data points show range for individual photoelectrons from successive pulses spaced at 3.5-sec intervals.

Since the expanded record provided an accurate determination of the time emission of individual photoelectrons, it was possible to follow changes in the height of the cloud for a short period before the rapidly increasing sky background made it difficult to distinguish between the spikes associated with echoes from a geometrically thin scattering layer and randomly spaced noise spikes, without employing a considerable amount of imagination. Figure VII-13 shows measured ranges for spikes between 72 km and 77 km for 25 consecutive traces obtained at 3.5-sec intervals on 6-7 July. The first trace corresponds to the time when visual observations suggested that the cloud was directly overhead (and is also the first trace in the series for deriving Fig. VII-12). Unfortunately, the noise increased too rapidly after this short sequence to distinguish the NLC echoes. This short record does indicate, however, a wave structure with a vertical amplitude of ~2 km and a horizontal wavelength corresponding to a transit time of approximately 3 minutes.

G. Fiocco, G. W. Grams

References

1. G. Fiocco and G. W. Grams, "Observations of the Upper Atmosphere by Optical Radar in Alaska and Sweden during the Summer 1964," Tellus 18, 34-38 (1966).
2. G. Fiocco and G. W. Grams, "Observations of the Aerosol Layer at 20 km by Optical Radar," J. Atmos. Sci. 21, 323-324 (1964).
3. G. W. Grams and G. Fiocco, "The Stratospheric Aerosol Layer during 1964 and 1965" (to appear in J. Geophys. Res., Vol. 72, 1967).
4. J. E. McDonald, "Atmospheric Exclusion Limits for Clouds of Water and Other Substances," J. Geophys. Res. 69, 3669-3672 (1964).
5. G. F. Schilling, "Forbidden Regions for the Formation of Clouds in a Planetary Atmosphere," J. Geophys. Res. 69, 3663-3667 (1964).